2011 IEEE/RSJ International Conference on
Intelligent Robots and Systems
September 25-30, 2011. San Francisco, CA, USA

Design, Modeling, Estimation and Control for Aerial Grasping and Manipulation

Daniel Mellinger, Quentin Lindsey, Michael Shomin and Vijay Kumar

Abstract— **This paper addresses mechanics, design, estimation and control for aerial grasping. We present the design of several light-weight, low-complexity grippers that allow quadrotors to grasp and perch on branches or beams and pick up and transport payloads. We then show how the robot can use rigid body dynamic models and sensing to verify a grasp, to estimate the the inertial parameters of the grasped object, and to adapt the controller and improve performance during flight. We present experimental results with different grippers and different payloads and show the robot's ability to estimate the mass, the location of the center of mass and the moments of inertia to improve tracking performance.**

I. Introduction

In recent years, we have seen extensive research on unmanned aerial vehicles (UAVs) [19], [6], [8], [4]. UAVs offer promises of speed and access to regions that are otherwise inaccessible to ground robotic vehicles. Although most UAV research has focused on fixed-wing aerial vehicles, rotorcrafts such as quadrotors have important benefits. These vehicles can be scaled down to small sizes and can operate in closed, confined environments such as inside buildings. With the smaller size comes increased agility and the ability to adapt to the environment. Micro UAVs can enter buildings, obtain information in environments that are dangerous for humans, and perch on walls or on joists for monitoring and surveillance.

However, most research on UAVs has typically been limited to monitoring and surveillance applications where the objectives are limited to "look" and "search" but "don't touch." Indeed contact with the environment is avoided as UAVs are primarily used for fly-throughs, such as surveillance and search and rescue. Thus the underlying research focuses on navigation and observation of the environment while minimizing interactions with that environment. By allowing UAVs, specifically quadrotors, to interact with the environment, we get an entire new set of applications.

First, allowing robots to fly and perch on rods or beams allows them to increase the endurance of their missions. Indeed, if perches are equipped with charging stations, robots can recharge their batteries extending their lives substantially. Second, the ability to grasp objects allows robots to access payloads that are unavailable to ground robots. There are fewer workspace constraints for aerial robots. Third, as our previous work shows, robots are able to assemble structures and scaffolds of arbitrary height in three dimensions without requiring such special purpose structures as tower cranes.

D. Mellinger, Q. Lindsey, M. Shomin and V. Kumar are with the Department of Mechanical Engineering and Applied Mechanics, University of Pennsylvania, Philadelphia, PA 19104, USA {dmel, quentinl, shomin, kumar}@seas.upenn.edu

There are many challenges in aerial grasping for micro UAVs. The biggest challenge arises from their limited payload. While multiple robots can carry payloads with grippers [15] or with cables [16], their end effectors and grippers have to be light weight themselves and capable of grasping complex shapes. Second, the dynamics of the robot are significantly altered by the addition of payloads. Indeed this is also an attraction in assembly because aerial robots can use this to sense disturbance forces and moments. However, for payload transport, it is necessary that the robots be able to estimate the inertia of the payload and adapt to it to improve tracking performance.

This paper addresses the mechanics, design and control for aerial grasping. The next section presents the background literature in relevant areas. In Sec. III several grippers we have developed for aerial grasping are described. Section IV explains the dynamic model and control strategy. Section V discusses parameter estimation methods and their application to the quadrotor dynamics. Finally, we present experimental results in Sec. VI.

II. Background

a) Aerial Manipulation: Aerial manipulation with full-size helicopters using cables is performed extensively in several applications. The logging industry uses helicopters to transport logs and equipment from areas that trucks cannot access while power companies use this approach to transport and assemble transmission line towers in remote areas. Smaller size rotorcraft have also been used with cables to manipulate objects. The authors of [3] designed a simplified model for modeling single/multiple small size helicopters, objects and ropes. In [16], the authors focused on position and orientation control of a towed object in 6 dimensions by treating multiple quadrotors as anchors whose positions could be controlled in three dimensions.

In contrast to aerial towing, direct manipulation using grippers can be used to manipulate objects aerially. In [20], the authors develop an elastic constraint contact model to study the flight stability of a small RC helicopter with a compliant gripper in contact with an object and/or the ground. In our previous work [11], [15], we used grippers described in Sec. III to pick up parts and explored multi-robot cooperative transport requiring grasping. None of this previous work, however, considers the changes in flight dynamics due to the grasped payload.

b) Quadrotor Control: Quadrotor control has been widely addressed in the literature from basic hovering and trajectory following [8], [4] to aggressive and aerobatic maneuvers [12], [13] . However, in nearly all previous

978-1-61284-455-8/11/$26.00 ©2011 IEEE

(a) The beam is grasped with an impactive gripper.

(b) The flat piece of wood is held by an ingressive gripper.

Fig. 1. Quadrotors carrying objects

work the dynamic model is considered to be known and in most cases, the center of mass is assumed to be coincident with the geometric center of the quadrotor. We depart from that paradigm in this work by explicitly accounting for the center of mass offset in the controller described in Sec. IV and allowing the mass of the robot+payload system to be unknown.

c) Parameter Estimation: Estimation of unknown parameters in dynamic systems is a problem of great interest in robotics. A common approach is to use linear least-squares methods in systems where the unknown parameters are linear in the equations of motion. These approaches have been applied in a number of systems from robotic manipulators [7] to underwater vehicles [5]. We will adopt a similar strategy for estimating the unknown parameters that change when a quadrotor transports payloads.

d) Aerial Robot Platform: All the methods that will be described are implemented on the Hummingbird quadrotor purchased from Ascending Technologies [1]. In our work, as in [17], the high-level position control loop for autonomous operation runs on a control computer that receives the quadrotor pose estimates from VICON. Interprocess communication on the control computer is handled by ROS [21] and a ROS-MATLAB bridge [2]. The control computer sends inputs to the ARM7 processor on the quadrotors via XBEE at a fixed rate of 100 Hz, which runs the low-level attitude control loop and computes the desired motor speeds.

III. GRIPPER DESIGN

In our previous work with quadrotors, we have used impactive and ingressive methods of grasping. Impactive grippers use solid jaws or fingers in contact with an object to produce the necessary grasping force while ingressive grippers depend on surface deformation, possibly penetration of the surface, to grasp the object [18].

1) Impactive Gripper: Impactive grippers typically use clamping motions either to enclose or to apply sufficient normal forces and by extension frictional forces to the walls of the object to overcome gravity. In general, these clamping motions are easy to generate using singly actuated mechanisms, which can alleviate weight concerns. Impactive grippers are particularly useful when the gripper can be designed for a small set of parts and orientations such as the gripper shown Fig. 1(a) used for assembling structures with quadrotors [11]. Although this impactive gripper was designed to carry specific parts it can also grasp a wider range of objects.

2) Ingressive Grippers: Impactive grippers require that the object's dimensions are compatible with the gripper's geometry. In contrast, ingressive grippers excel at handling

(a) Actively Engaging

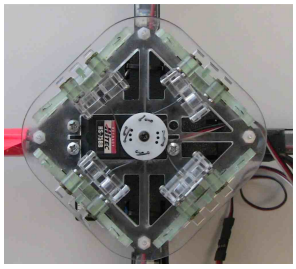

(b) Passively Engaging

Fig. 2. Ingressive Grippers

objects that do not have well-defined attachment points which are made of wood, foam, fabric or other porous or deformable materials. The ingressive grippers shown in Fig. 2 use the paradigm of penetration into surfaces with metal hooks to attach to surfaces. They use opposing hooks which allows for large normal forces with respect to the penetration force. In previous work [14], [15], we presented an actively engaging gripper shown in Fig. 2(a) in which a servo drives the hooks into a surface. Here, we present a new design shown in Figs. 1(b) and 2(b) in which the hooks passively engage in a surface.

When the surface contacts the center pin in the loaded state (Fig. 3(a)), the clips in the preloaded flex arms are released and the spring force causes them to move to the closed configuration (Fig. 3(b)), which engages the hooks into the material. The planar mechanism in Fig. 3 is repeated four times around the central axis of the quadrotor, as seen in Fig. 2(b). This provides a number of attachment points and compensates for problems associated with the grain of attachment medium. To disengage the gripper from the surface, a servo mechanism show in Fig. 2(b) releases a lock in each of the four planar mechanisms. By pulling the lock out of the plane, the preloaded springs release and pull the hooks away from the surface as shown in Fig. 3(c).

For both grippers Shape Deposition Manufacturing (SDM), a technique especially useful for polymers, is employed to manufacture the compliant component of the gripper [22]. A negative mold of the compliant part is CNC-machined into a machinable wax. Predefined geometries allow the hooks to be located exactly in the mold so that angle of attack of the hooks is consistent. A two part epoxy-resin material is poured into the negative, cured and released from the mold. These parts are assembled with additional laser-cut acrylic parts and Hitec HS-81 servos to complete the grippers.

IV. QUADROTOR DYNAMICS AND CONTROL

When the grippers described in the previous section are used to transport objects the dynamic model of the quadrotor changes. We describe the dynamic model and control strategy in this section.

A. Dynamic Model

The coordinate systems including the world frame, $\mathcal{W}$, and body frame, $\mathcal{B}$, as well as the free body diagram for the quadrotor are shown in Fig. 4. We use $Z-X-Y$ Euler angles to define the roll, pitch, and yaw angles (ϕ, θ, and ψ). The rotation matrix from $\mathcal{B}$ to $\mathcal{W}$ is given by ${}^{W}R_{B}$. The angular

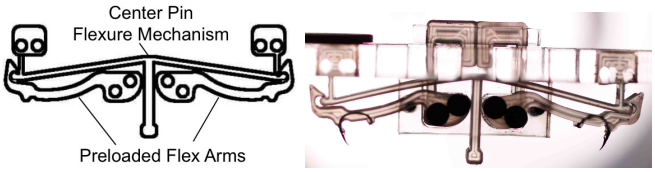

(a) Preloaded, open gripper with clips engaged

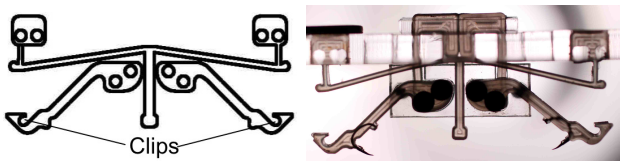

(b) Closed gripper with clips released

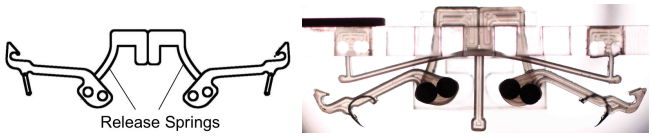

(c) Hooks retracted by preloaded release springs

Fig. 3. Passively engaging ingressive gripper details

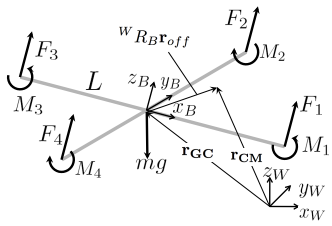

Fig. 4. Free Body Diagram and Coordinate Systems

velocity of the robot is denoted by ω, denoting the angular velocity of frame $\mathcal{B}$ in the frame $\mathcal{W}$, with components p, q, and r in the body frame. Each rotor has an angular speed ω_i and produces a force F_i and moment M_i according to

$$F_i = k_F \omega_i^2, \; M_i = k_M \omega_i^2.$$

Since the motor dynamics are fast compared to the rigid body dynamics and the aerodynamics, we will assume that rotor speeds can be instantly achieved during the controller development. Therefore, the control input $\mathbf{u}$, where u_1 is the net body force and u_2, u_3, u_4 are the body moments, can be expressed in terms of the rotor speeds as

$$\mathbf{u} = \begin{bmatrix} k_F & k_F & k_F & k_F \\ 0 & k_F L & 0 & -k_F L \\ -k_F L & 0 & k_F L & 0 \\ k_M & -k_M & k_M & -k_M \end{bmatrix} \begin{bmatrix} \omega_1^2 \\ \omega_2^2 \\ \omega_3^2 \\ \omega_4^2 \end{bmatrix}, \qquad (1)$$

where L is the distance from the axis of rotation of the rotors to the center of the quadrotor.

The position vector of the center of mass and geometric center $\mathbf{r}_{CM}$ and $\mathbf{r}_{GC}$, respectively, are related according to

$$\mathbf{r}_{CM} = \mathbf{r}_{GC} + {}^W R_B \mathbf{r}_{\text{off}},$$

where $\mathbf{r}_{\text{off}} = [x_{\text{off}}, y_{\text{off}}, z_{\text{off}}]^T$ are offsets in body-frame coordinates.

The forces on the system are gravity, in the $-z_W$ direction, and $u_1 = \sum F_i$, in the z_B direction where F_i is the force from each rotor. Newton's equations of motion governing the acceleration of the geometric center are

$$m\left(\ddot{\mathbf{r}}_{GC} + \alpha \times \mathbf{r}_{\text{off}} + \omega \times (\omega \times \mathbf{r}_{\text{off}})\right) = -mg\mathbf{z}_W + u_1 \mathbf{z}_B, \qquad (2)$$

where α is the angular acceleration of frame $\mathcal{B}$ in frame $\mathcal{W}$.

The Euler equation for the system is

$$\mathcal{I}_{CM}\dot{\omega} = -\omega \times \mathcal{I}_{CM}\omega + \begin{bmatrix} u_2 \\ u_3 \\ u_4 \end{bmatrix} - \mathbf{r}_{\text{off}} \times \begin{bmatrix} 0 \\ 0 \\ u_1 \end{bmatrix} \qquad (3)$$

where $\mathcal{I}_{CM}$ is the moment of inertia matrix referenced to the center of mass along the $x_B - y_B - z_B$ axes. Note that the net propeller force, u_1, creates a moment in (3) since u_1 acts at the geometric center which is not coincident with the center of mass.

B. Quadrotor Control

We now present a controller to follow specified near-hover trajectories in position of the geometric center and yaw angle, $\mathbf{r}_T(t)$ and $\psi_T(t)$. First, we define the errors on position and velocity as

$$\mathbf{e}_p = \mathbf{r}_{GC} - \mathbf{r}_T, \; \mathbf{e}_v = \dot{\mathbf{r}}_{GC} - \dot{\mathbf{r}}_T.$$

Next we compute the desired force vector:

$$\mathbf{F}_{des} = -K_p\mathbf{e}_p - K_i \int \mathbf{e}_p - K_v\mathbf{e}_v + \hat{m}g\mathbf{z}_W + \hat{m}\ddot{\mathbf{r}}_T,$$

where K_p, K_i, and K_v are positive definite gain matrices and $\hat{m}$ is the estimate of the system mass. Note that this controller effectively treats the two terms $m\alpha \times \mathbf{r}_{\text{off}}$ and $m\omega \times (\omega \times \mathbf{r}_{\text{off}})$ in (2) as disturbances that are rejected by the feedback. This is done because these terms are generally small relative to the other terms in practice.

The magnitude of the desired force vector $\mathbf{F}_{des}$ is the first control input, u_1. The desired roll and pitch angles, ϕ_{des} and θ_{des}, are found by determining the attitude which achieves the desired lateral components of $\mathbf{F}_{des}$ for the desired yaw angle ψ_T. The net body frame moments are then computed according to:

$$\begin{bmatrix} u_2 \\ u_3 \\ u_4 \end{bmatrix} = K_R \begin{bmatrix} \phi_{des} - \phi \\ \theta_{des} - \theta \\ \psi_T - \psi \end{bmatrix} - K_\omega \begin{bmatrix} p \\ q \\ r \end{bmatrix} + \begin{bmatrix} \hat{y}_{\text{off}} u_1 \\ -\hat{x}_{\text{off}} u_1 \\ 0 \end{bmatrix},$$

where K_R and K_ω are diagonal gain matrices and $\hat{x}_{\text{off}}$ and $\hat{y}_{\text{off}}$ are estimates of the center of mass offsets. Finally we compute the desired rotor speeds to achieve the desired $\mathbf{u}$ by inverting (1).

The departure from previous work [13], [17], is that we explicitly include our estimates of the mass of the system and center of mass offsets in the controller, these changes can be significant during payload transport. The offset causes pitching and rolling moments that change with the net thrust produced. Explicitly including this term leads to significantly improved tracking performance as shown in Sec. VI.

V. Estimation of Inertial Parameters

A. Least-squares method for parameter estimation

We use methods which require the unknown parameters, θ, to appear linearly in the equations of motion [10], [9]. We will allow p equations to contain these unknown parameters. We use Tustin's method to convert the differential equations of motion to discrete time equations which can be written as

$$y_j(k+1) = \theta^T \phi_j(k)$$

where k represents the time step, θ is the *parameter vector*, ϕ_j and y_j are the *measurement vector* and system output for equation j. The goal is to find an *estimated parameter vector*, $\hat{\theta}$.

We use least-squares methods to estimate the unknown parameter vectors. The cost function to be minimized is

$$\min_{\hat{\theta}(k)} J(k) = \sum_{i=1}^{k} \lambda_1^{(k-i)} \sum_{j=1}^{p} \left(y_j(i) - \hat{\theta}^T(k)\phi_j(i-1) \right)^2$$

where $\lambda_1 \leq 1$ is a *forgetting factor* which is used to weight old data less than new data. Here the cost function is a function of the squared error over k time steps and the p equations. Note that this cost function can be minimized in a batch fashion or recursively [10].

1) Batch Least-Squares: The solution to the batch least-squares problem with a forgetting factor of 1 for data collected over k time steps is

$$\theta_{LS} = \hat{R}_{\phi\phi}^{-1} \hat{r}_{\phi y}$$

where

$$\hat{R}_{\phi\phi} = \frac{1}{kp} \sum_{i=1}^{k} \sum_{j=1}^{p} \phi_j(i-1)\phi_j(i-1)^T$$

and

$$\hat{r}_{\phi y} = \frac{1}{kp} \sum_{i=1}^{k} \sum_{j=1}^{p} \phi_j(i-1) y_j(i)$$

2) Recursive Least-Squares: The method can also be applied recursively so that the estimate changes at each time step as new data is received. In this case the parameter vector estimate is updated according to:

$$\hat{\theta}(k+1) = \hat{\theta}(k) + F(k+1) \sum_{j=1}^{p} \phi_j(k) \epsilon_j^0(k+1)$$

where

$$\epsilon_j^0(k+1) = y_j(k+1) - \hat{\theta}^T(k)\phi_j(k).$$

Here $F(k)$ is a weight matrix that is also recursively updated based of the inversion of:

$$F(k)^{-1} = \lambda_1 F(k+1)^{-1} + \sum_{j=1}^{p} \phi_j(k)\phi_j(k)^T \qquad (4)$$

3) Persistent Excitation: Both approaches require ϕ_j to be *persistently exciting*. The measurement vectors, ϕ_j, are persistently exciting if

$$\lim_{k_1 \to \infty} \frac{1}{k_1} \sum_{i=1}^{k_1} \sum_{j=1}^{p} \phi_j(i)\phi_j(i)^T > 0.$$

Intuitively, this conditions means that the dynamics are excited sufficiently to identify the unknown parameters. In the batch least-squares method, persistent excitation guarantees that $\hat{R}_{\phi\phi}$ is invertible. In the recursive least-squares method, we see from (4) that if the term $\sum_{j=1}^{p} \phi_j(k)\phi_j(k)^T$ becomes non full rank then the adaptive gain, $F(k)$, will tend towards infinity if the forgetting factor, λ_1, is less than one.

B. Application to Quadrotor Dynamics

These least-squares methods parameter estimation methods are applied to the equations of motion of the quadrotor as described here.

1) Estimation of payload parameters during hover: When the quadrotor is commanded to hover in place the derivatives of the position and Euler angles are nominally zero. Eliminating these terms from the equations of motion simplifies the parameter estimation method. Consider the z equation of motion during hover:

$$0 = u_1 \left(\mathbf{z}_B \cdot \mathbf{z}_W \right) - mg.$$

Treating m as the unknown parameter and applying the batch least-squares method for k measurements yields

$$\hat{m} = \frac{1}{gk} \sum_{i=1}^{k} u_1(i) \left(\mathbf{z}_B(i) \cdot \mathbf{z}_W \right).$$

Next we consider the Euler equation for the y axis during hover treating the net body force as a known constant, $\bar{u}_1$, where barred coordinates represent the average over the time span of collected data. The unknown offset, x_{off}, found via least-squares is simply an average over collected data:

$$\hat{x}_{\text{off}} = \frac{\bar{u}_3}{\bar{u}_1}.$$

The y axis offset is found similarly. Note the moments of inertia cannot be found during hover because the terms multiplying them are zero. An experimental benefit to this approach is that averages can be computed on the onboard controller and sent back to a control computer at a slower rate than what is required for the method described in Sec. V-B.3 where applied moments and angular velocities are constantly changing. Note that this method assumes that the robot is not being subjected to any disturbances.

2) Estimation of payload mass in the presence of disturbances: Newton's equations provide three equations which give information about the mass of the system:

$$\begin{aligned} m\ddot{x} &= u_1 \left(\mathbf{z}_B \cdot \mathbf{x}_W \right) + F_x \\ m\ddot{y} &= u_1 \left(\mathbf{z}_B \cdot \mathbf{y}_W \right) + F_y \\ m\ddot{z} &= u_1 \left(\mathbf{z}_B \cdot \mathbf{z}_W \right) - mg \end{aligned}$$

where F_x and F_y are the lateral aerodynamic disturbance forces.

In this formulation the unknown parameter vector is $\theta = [1/m, F_x/m, F_y/m]^T$. Since the mass of the quadrotor and gripper are fixed this method can be used to determine the mass of the payload. The recursive least-squares method can run in real-time and is especially useful for identifying if the quadrotor has successfully picked up or dropped payload.

3) Estimation of payload inertia: The Euler equations for a system in which the center of mass is offset from the geometric center by some vector $\mathbf{r}_{\text{off}}$ are given by (3). We make two assumptions to make these nonlinear equations suitable for our parameter estimation methods: (1) the body axes of the quadrotor are close to the principal axes so its products of inertia are small and (2) the excitation is primarily about one axis so the $\omega \times (I \times \omega)$ term can be neglected. Under these assumptions the equation of motion about the y axis is

$$I_{yy}\dot{q} = u_3 + u_1 x_{\text{off}},$$

where u_1 is the net body force from the props, u_3 is the applied moment along the y axis, and x_{off} is the center of mass offset in the x direction. Here the unknown parameter vector is $\theta = [1/I_{yy}, x_{\text{off}}/I_{yy}]^T$. The least-squares estimators

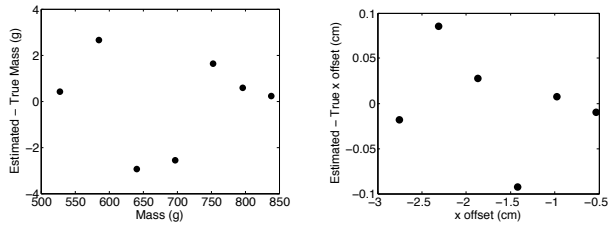

(a) Changing Mass (b) Changing x offset

Fig. 5. Data for mass and center of mass offset during hover.

can be applied using flight data for which the pitch dynamics are sufficiently excited. An equivalent procedure is used along for the z and x axes to estimate I_{zz}, I_{xx}, and y_{off}.

VI. Experimental Results

A. Estimation of payload parameters during hover

Mass was incrementally added to the system, and the quadrotor was commanded to hover in place for about 10 seconds for each condition. The mass of the system was estimated with the method described in Sec. V-B.1 as shown in Fig. 5(a). The average net thrust was computed by averaging the commanded net thrust sent from the control computer. Note that the error in the prediction is less than 3 grams in all cases.

A mass of 66 grams was added to a quadrotor weighing 687 grams at a number of positions along the x axis in order to offset the center of mass. The theoretical change in the center of mass and the error in estimated center of mass offset are shown in Fig. 5(b). Note that the error in the center of mass position estimate is less than 1 mm in all cases. The average net thrust was computed as described above and the average moments were computed by averaging the commanded moments on the onboard microprocessor and sending out these averages at a rate of 10 Hz. Sending out data at a low rate allowed the quadrotor to be computer controlled via the same XBEE module.

B. Estimation of payload mass in the presence of disturbances

The procedure described in Sec. V-B.2 was applied in a scenario where the quadrotor was commanded to pick up three payloads of different mass and drop them at a prescribed location. For this estimator the accelerations were computed by numerical differentiating the position estimates from VICON. The applied forces were calculated from the commanded net thrust and the orientation sensed from VICON. Since the mass changes in this experiment the recursive least-squares method was used. The estimated mass during this experiment along with the true mass is shown in Fig. 6. As expected, the estimated disturbance forces (not shown) are small. For this data a forgetting factor, λ_1, of 0.985 was used. Choosing a larger forgetting factor makes the mass estimate less noisy but at the cost of responding slower to changes in system parameters.

C. Estimation of payload inertia

The procedure described in Sec. V-B.3 was implemented on the quadrotor. For this estimator the angular accelerations were computed by numerically differentiating the

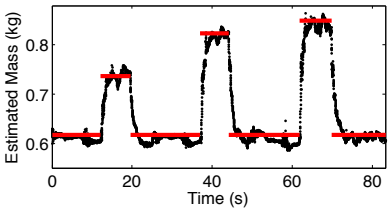

Fig. 6. Mass estimate (black) and true mass (red) for quadrotor picking up and dropping of three payloads with different weights. The pick up and drop off events can be observed from the change in the true mass.

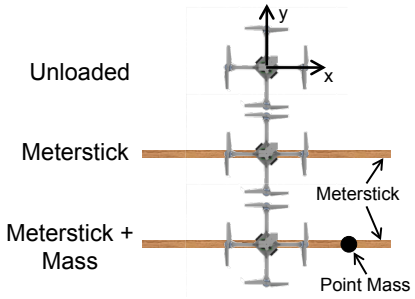

Fig. 7. Three loading cases tested. The meterstick weighs 125 grams and the point mass weighs 66 grams.

angular velocities sensed by the 3-axis rate gyro onboard the quadrotor. The commanded body moments and net force are also available on the onboard controller. In the current experimental setup, it is impossible to both send and receive commands at high rates using a single XBEE module. For this reason in these experiments, the quadrotor was commanded by a pilot using the RC, and the XBEE was used to send data out at a rate of 100 Hz.

This method was applied for the three cases shown in Fig. 7. For the last case the point mass is offset from the center of mass by 30 cm in the x direction. For each case, the pilot commanded oscillatory excitation about each of the three axes independently. Data for the pitch excitation for the *Unloaded* and *Meterstick + Mass* cases are shown in Fig. 8. Note that the larger moment of inertia can observed from the larger moment in (b) required to produce less angular acceleration. Also, the center of mass offset can be observed from the nonzero mean moment required in (b).

As shown in Table I, the batch least-squares method was applied to estimate the unknown parameters for each combination of case and axis. Note that the y axis offset remain unchanged as expected. For the *Meterstick + Mass* case the x axis offset increases by about 3.2 cm. Theoretically, it should increase by about 2.6 cm. The inertia estimates behave qualitatively as expected. The moment of inertia along the x axis increases slightly for the added payloads. As expected, significant increases in I_{yy} and I_{zz} are observed for the added payloads.

D. Controller Compensation

The gripper was loaded with a 120 gram horizontal beam as far to one side as possible in the $-x$ direction as shown in Fig. 1(a). The mass and center of mass were estimated using the methods described in Sec. V-B.1 using 3 seconds of data collected while hovering in place. The quadrotor was then commanded to fly along a sine wave along the z-

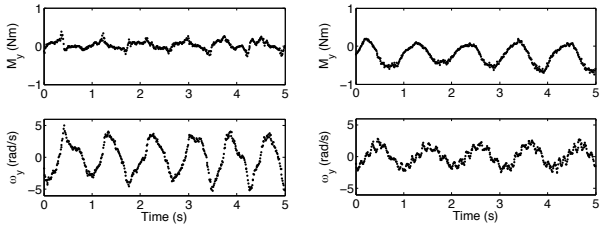

(a) Unloaded Case (b) Meterstick + Mass Case

Fig. 8. Pitch Moment and Pitch Angular Velocity Data

Case	I_{xx}	I_{yy}	I_{zz}	x_{off}	y_{off}
Unloaded	3.9	4.4	4.9	-0.30	0.12
Meterstick	5.2	21.5	15.3	-0.26	0.12
Meterstick + Mass	5.8	32.6	21.9	2.89	0.13

TABLE I

IDENTIFIED PROPERTIES (ALL INERTIAS IN gm^2 AND LENGTHS IN cm)

axis with amplitude 0.767 meters and frequency 2.77 rad/s using the compensated and uncompensated controller. The compensated controller used the estimated mass and center of mass offset while the uncompensated controller assumed the offset to be zero and the mass to be the mass of the quadrotor and gripper with no part. Plots of the errors in the x and z directions as well as their standard deviations are shown in Fig. 9. Note that the x performance is in the direction of the center of mass offset. Including the estimated parameters leads to significantly improved tracking performance for this trajectory. This improvement will be significant whenever the trajectory calls for significant changes in the thrust commanded since a changing thrust causes a changing moment which is explicitly cancelled using the controller described here.

VII. CONCLUDING REMARKS

Picking up and transporting payload is a valuable capability for unmanned aerial vehicles. We have demonstrated the ability to grasp and manipulate a number of items using quadrotor helicopters with several grippers that we have designed. When quadrotors transport objects important flight parameters change. Methods for identifying the mass, center of mass offset, and moments of inertia using batch and recursive least-squares methods were described in this paper. A controller was described which explicitly accounts for the estimated mass and center of mass offset. Experimental data was presented to demonstrate all parameter estimation methods. Significant improvement in tracking performance was shown with the inclusion of the estimated parameters.

VIII. ACKNOWLEDGEMENTS

We gratefully acknowledge support from ONR Grants N00014-07-1-0829 and N00014-09-1-1051, and ARL Grant W911NF-08-2-0004.

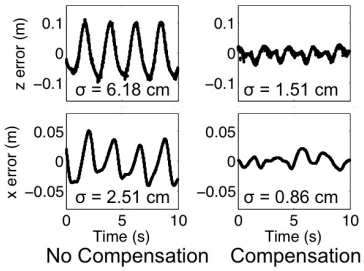

Fig. 9. Time histories and standard deviations of x and z errors for uncompensated and compensated controller for following the trajectory $z(t) = 0.77\sin(2.77t)m$ with x and y constant for 10 seconds.

REFERENCES

[1] Ascending Technologies, GmbH. http://www.asctec.de.

[2] ROS-Matlab Bridge. http://github.com/nmichael/ipc-bridge.

[3] M. Bernard and K. Kondak. Generic slung load transportation system using small size helicopters. In *In Proceedings of the IEEE International Conference on Robotics and Automation*, pages 3258–3264, 2009.

[4] S. Bouabdallah. *Design and Control of Quadrotors with Application to Autonomous Flying*. PhD thesis, Ecole Polytechnique Federale de Lausanne, 2007.

[5] M. Caccia, G. Indiveri, and G. Veruggio. Modeling and identification of open-frame variable configuration unmanned underwater vehicles. *Oceanic Engineering, IEEE Journal of*, 25(2):227 –240, Apr. 2000.

[6] G. Cai, B. Chen, and T. Lee. An overview on development of miniature unmanned rotorcraft systems. *Frontiers of Electrical and Electronic Engineering in China*, 5:1–14, 2010. 10.1007/s11460-009-0065-3.

[7] G. Calafiore, M. Indri, and B. Bona. Robot dynamic calibration: Optimal excitation trajectories and experimental parameter estimation. *Journal of Robotic Systems*, 18(2):55–68, 2001.

[8] G. Hoffmann, S. Waslander, and C. Tomlin. Quadrotor helicopter trajectory tracking control. In *AIAA Guidance, Navigation and Control Conference and Exhibit*, Honolulu, Hawaii, Apr. 2008.

[9] P. Ioannou and B. Fidan. *Adaptive Control Tutorial*. SIAM: Society for Industrial and Applied Mathematics, 2006.

[10] I. D. Landau, R. Lozano, and M. M'Saad. *Adaptive Control*. Springer, 1998.

[11] Q. Lindsey, D. Mellinger, and V. Kumar. Construction of cubic structures with quadrotor teams. *Robotics: Science and Systems*, 2011.

[12] S. Lupashin, A. Schollig, M. Sherback, and R. D'Andrea. A simple learning strategy for high-speed quadrocopter multi-flips. In *Proc. of the IEEE Int. Conf. on Robotics and Automation*, pages 1642–1648, Anchorage, AK, May 2010.

[13] D. Mellinger, N. Michael, and V. Kumar. Trajectory generation and control for precise aggressive maneuvers with quadrotors. In *Int. Symposium on Experimental Robotics*, New Delhi, India, Dec. 2010.

[14] D. Mellinger, M. Shomin, and V. Kumar. Control of quadrotors for robust perching and landing. In *Proceedings of the International Powered Lift Conference*, Oct 2010.

[15] D. Mellinger, M. Shomin, N. Michael, and V. Kumar. Cooperative grasping and transport using multiple quadrotors. In *International Symposium on Distributed Autonomous Systems*, Lausanne, Switzerland, November 2010.

[16] N. Michael, J. Fink, and V. Kumar. Cooperative manipulation and transportation with aerial robots. *Autonomous Robots*, 30:73–86(14), January 2011.

[17] N. Michael, D. Mellinger, Q. Lindsey, and V. Kumar. The grasp multiple micro uav testbed. *IEEE Robotics and Automation Magazine*, Sept 2010.

[18] G. Monkman, S. Hesse, R. Steinmann, and H. Schunk. *Robot Grippers*. Wiley, Berlin, 2007.

[19] D. Pines and F. Bohorquez. Challenges facing future micro air vehicle development. *AIAA Journal of Aircraft*, 43(2):290–305, 2006.

[20] P. Pounds and A. Dollar. Hovering stability of helicopters with elastic constraints. In *ASME Dynamic Systems and Control Conference*, 2010.

[21] M. Quigley, K. Conley, B. P. Gerkey, J. Faust, T. Foote, J. Leibs, R. Wheeler, and A. Y. Ng. Ros: an open-source robot operating system. In *ICRA Workshop on Open Source Software*, 2009.

[22] L. E. Weiss, R. Merz, F. B. Prinz, G. Neplotnik, P. Padmanabhan, L. Schultz, and K. Ramaswami. Shape deposition manufacturing of heterogeneous structures. *Journal of Manufacturing Systems*, 16(4):239 – 248, 1997.